

Phase sensitive sensor on Tamm plasmon devices

SYUAN-GUEI HUANG, KUO-PING CHEN, AND SHIE-CHANG JENG*

Institute of Imaging and Biomedical Photonic, National Chiao Tung University, Tainan 711, Taiwan
*scjeng@faculty.nctu.edu.tw

Abstract: This work proposes a refractive index sensing concept of a Tamm plasmon (TP) device by using spectroscopic ellipsometry and phase detection. A TP device is generally composed of a 1-D photonic crystal (PC) with a metallic film on top of it. We found that the sensing performance can be improved by adjusting the parameters of the incident angle of polarized light, the top layer thickness, and the central wavelength of the PC. By designing proper parameters, it was found that the change of the phase difference of p-polarized and s-polarized lights, $\delta\Delta$, can reach 34° when the ambient environment is changed from air ($n = 1.00028$) to carbon dioxide ($n = 1.00045$). A sensitivity of $\delta\Delta/\delta n \sim 2 \times 10^5$ °/RIU can then be obtained for the proposed TP device.

© 2017 Optical Society of America

OCIS codes: (240.6680) Surface plasmons; (240.2130) Ellipsometry and polarimetry.

References and links

1. K. Kneipp, H. Kneipp, I. Itzkan, R. R. Dasari, and M. S. Feld, "Surface-enhanced Raman scattering and biophysics," *J. Phys. Condens. Matter* **14**(18), 202 (2002).
2. J. Homola, S. S. Yee, and G. Gauglitz, "Surface plasmon resonance sensors: review," *Sens. Actuators B Chem.* **54**(1-2), 3–15 (1999).
3. K. Y. Kim, *Plasmonics - Principles and Applications* (InTech, 2012).
4. M. Kaliteevski, I. Iorsh, S. Brand, R. A. Abram, J. M. Chamberlain, A. V. Kavokin, and I. A. Shelykh, "Tamm plasmon-polaritons: Possible electromagnetic states at the interface of a metal and a dielectric Bragg mirror," *Phys. Rev. B* **76**(16), 165415 (2007).
5. W. L. Zhang and S. F. Yu, "Bistable switching using an optical Tamm cavity with a Kerr medium," *Opt. Commun.* **283**(12), 2622–2626 (2010).
6. C. Symonds, A. Lemaître, P. Senellart, M. H. Jomaa, S. Aberra Guebrou, E. Homeyer, G. Brucoli, and J. Bellessa, "Lasing in a hybrid GaAs/silver Tamm structure," *Appl. Phys. Lett.* **100**(12), 121122 (2012).
7. W. L. Zhang, F. Wang, Y. J. Rao, and Y. Jiang, "Novel sensing concept based on optical Tamm plasmon," *Opt. Express* **22**(12), 14524–14529 (2014).
8. B. Auguie, M. C. Fuertes, P. C. Angelomé, N. L. Abdala, G. J. A. A. Soler Illia, and A. Fainstein, "Tamm plasmon resonance in mesoporous multilayers: Toward a sensing application," *ACS Photonics* **1**(9), 775–780 (2014).
9. R. Das, T. Srivastava, and R. Jha, "Tamm-plasmon and surface-plasmon hybrid-mode based refractometry in photonic bandgap structures," *Opt. Lett.* **39**(4), 896–899 (2014).
10. R. B. M. Schasfoort and A. J. Tudos, eds., *Handbook of Surface Plasmon Resonance* (Royal Society of Chemistry, 2008).
11. A. V. Kabashin, S. Patskovsky, and A. N. Grigorenko, "Phase and amplitude sensitivities in surface plasmon resonance bio and chemical sensing," *Opt. Express* **17**(23), 21191–21204 (2009).
12. Y. Huang, H. P. Ho, S. K. Kong, and A. V. Kabashin, "Phase-sensitive surface plasmon resonance biosensors: methodology, instrumentation and applications," *Ann. Phys. (Berlin)* **524**(11), 637–662 (2012).
13. P. E. Ciddor, "Refractive index of air: new equations for the visible and near infrared," *Appl. Opt.* **35**(9), 1566–1573 (1996).
14. A. Bideau-Mehu, Y. Guern, R. Abjean, and A. Johannin-Gilles, "Interferometric determination of the refractive index of carbon dioxide in the ultraviolet region," *Opt. Commun.* **9**(4), 432–434 (1973).
15. The refractive index of gas depends on several parameters, such as pressure, temperature and wavelength. The values adopted in this work are only for theoretical calculation. However, the error is less than 5% for practical applications.
16. Database of Essential Macleod, viewed 6 February 2017.
17. O. Gazzano, S. Michaelis de Vasconcellos, K. Gauthron, C. Symonds, J. Bloch, P. Voisin, J. Bellessa, A. Lemaître, and P. Senellart, "Evidence for confined Tamm plasmon modes under metallic microdisks and application to the control of spontaneous optical emission," *Phys. Rev. Lett.* **107**(24), 247402 (2011).
18. H. Zhou, G. Yang, K. Wang, H. Long, and P. Lu, "Multiple optical Tamm states at a metal-dielectric mirror interface," *Opt. Lett.* **35**(24), 4112–4114 (2010).

19. C.-Y. Chang, Y.-H. Chen, Y.-L. Tsai, H.-C. Kuo, and K.-P. Chen, "Tunability and optimization of coupling efficiency in Tamm plasmon modes," *IEEE J. Sel. Top. Quantum Electron.* **21**, 4600206 (2015).
20. V. G. Kravets, F. Schedin, A. V. Kabashin, and A. N. Grigorenko, "Sensitivity of collective plasmon modes of gold nanoresonators to local environment," *Opt. Lett.* **35**(7), 956–958 (2010).

1. Introduction

Plasmonics has been a rapidly developing topic in photonics. It has provided many applications in biophotonics and chemistry [1,2]. A conventional surface plasmon (SP) polaritons are formed with a TM polarization at the boundary of metallic and dielectric media by using dispersion-matching devices, like gratings or prisms [3]. Tamm plasmon (TP), formed by a high refractive index/low refractive index alternate-layered photonic crystal (PC) coated with a metallic film, can be easily excited by both the TE and TM polarization without using additional dispersion optics [4], therefore it is more convenient for practical applications. TP has been applied in many photonic devices, such as optical switches and semiconductor lasers [5,6]. Recently, a novel method of refractive index sensing using a high-refractive-index-contrast TP structure is proposed theoretically by Zhang *et al.* [7]. The presence of air layers in their proposed TP structure, an air/dielectric alternate-layered PC, increases the refractive index contrast of the PC and greatly enhances the sensor sensitivity by measuring the shift of resonance wavelength with the change of ambient refractive index. However, the air layers in TP structure are not easy to fabricate for practical applications. A complicated approach by using mesoporous multilayers has also been proposed recently to solve this issue [8]. Recently, the TM polarized hybrid mode formed as a consequence of coupling between TP polariton and SP polariton has been proposed and it exhibits a sensitivity ~ 900 nm/RIU [9]. Conventional SP resonance (SPR) has been extensively explored for sensors based on detection of amplitude characteristics [10]. In order to improve the detection sensitivity, the phase-sensitive SPR has been adopted due to the existence of an abrupt phase change under suitable SPR parameters [11]. Several techniques based on phase-sensitivity measurements have been demonstrated, such as SPR polarimetry and optical heterodyning [11,12].

In this work, the approach of spectroscopic ellipsometry (SE) was applied to measure the phase difference of p-polarized and s-polarized lights with the ambient refractive index for a TP device. By using a commercial software for theoretical modeling, it was found that the change of phase difference of p-polarized and s-polarized lights can reach 34° when the ambient environment is changed from air ($n = 1.00028$) to CO_2 ($n = 1.00045$) [13–15].

2. Structure design and analysis

The schematic of the proposed TP device and the apparatus for reflectance spectra measurement are shown in Figs. 1(a) and 1(b), respectively. A TP device is applied, using a standard quarter-wavelength PC composed of eight pairs of TiO_2 ($n \sim 2.30$ at 590 nm [16]) and SiO_2 ($n \sim 1.46$ at 590 nm [16]) with central wavelength $\lambda_c \sim 730$ nm. The thicknesses of the high (t_H) and low (t_L) refractive index films are given by $t_H = \lambda_c/4n_H$ and $t_L = \lambda_c/4n_L$, where n_H and n_L are the indices of refraction of the high and low index films, respectively. The TiO_2 and SiO_2 layers were deposited onto a glass substrate by the electron beam evaporation with the ion beam assisted deposition (Kingmate Tech. Co.). The thicknesses of TiO_2 and SiO_2 were ~ 78 and ~ 125 nm, respectively. The top-layer thickness of the TiO_2 , t_{TiO_2} , was ~ 239 nm. A gold film ~ 41 nm ($n = 0.24$, $k = 3.00$ at 590 nm [16]) was applied on the PC to form a TP device by using a thermal evaporator. For the measurement of reflectance spectra at normal incident, a white light illuminates the TP device from the metal side as shown in Fig. 1(b).

The ellipsometry spectra of the TP device placed in an ambient environment was measured by an ellipsometer (alpha-SE, J.A. Woollam Co.), and the light source illuminates the Tamm device from the metal side. The angle of incidence, θ_i , can be set at 65° , 70° or 75° . Ellipsometry is a very sensitive technique that applies p-polarized and s-polarized lights to

characterize the thin films. The polarization of light changes upon reflection. Then, the ellipsometry parameters

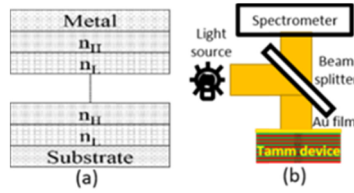


Fig. 1. (a) The schematic structure of the TP device, and (b) the apparatus for reflectance measurement.

ψ , describing the amplitude ratio, and the Δ , describing the phase difference of p-polarized and s-polarized lights are defined as

$$\frac{r_p}{r_s} = \frac{|r_p|}{|r_s|} e^{i(\delta_p - \delta_s)} = \tan(\psi) e^{i\Delta} \quad (1)$$

where r_s (r_p) is the s (p)-polarized complex reflection coefficient, and δ_s (δ_p) is the s (p)-polarized phase. The ψ and Δ can be measured by an ellipsometer. A commercial software, the Essential Macleod, is applied to simulate the SE parameters in this work. It has been shown that the resonance wavelength λ_{TP} of the TP device depends on the central wavelength of PC, λ_c , the t_{TiO_2} , and the metallic film [17–19]. It is worth to note that the sample structure, including the thickness and refractive index, cannot be identical between the theoretical design and the fabricated results. Although the λ_{TP} is changed with the thickness and refractive index of each film, we can determine the λ_{TP} from experimental results and design the measurement apparatus at proper conditions to improve the detection sensitivity with the aid of simulation. The contribution of this work is to discuss the effect to sensitivity from each different parameter and able to conclude a design rule to general TP sensors. The simulation was also applied to determine the apparent thickness for each film.

3. Results and discussion

Figure 2 shows the simulated and experimental reflectance spectra of the TP device at normal incidence. It is observed that λ_{TP} is at ~ 760 nm. The simulation shows good agreement to the experimental results. The deviation in resonance bandwidth is because of the optical loss in metal while doing thermal evaporation, like roughness and defects [17].

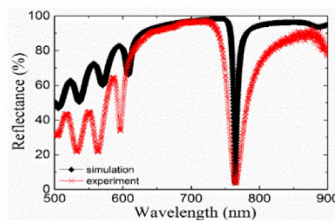


Fig. 2. Reflectance spectra of the simulation and experimental results for the TP device at normal incidence.

The experimental and simulation results of reflectance spectra, ψ and Δ for the TP device in the air environment at $\theta_i = 65^\circ$ are shown in Fig. 3, and a slight difference ~ 10 nm between them is observed. The difference of λ_{TP} , ~ 20 nm, between p and s polarized lights is also existed due to their different reflection properties. Two resonances in ψ are observed at about 660–700 nm, and two phase jumps in Δ take place at the same spectral points, corresponding to the two resonance minimums. The phase jump usually happens in the region of drop of

light intensity where phase is not defined, while the sharpness of phase jump is determined by the intensity of light in the resonance [11,12]. The sharp peak in Fig. 3(c) is because of the phase range is limited in 2π in the software. Therefore, at the λ_{TP} , the large Δ change will cause the step-like results. The dependences of Au thickness and θ_i on λ_{TP} , ψ and Δ are simulated and shown in Fig. 4 and Fig. 5, respectively. The results show that the 5 nm uncertainty for 40 nm Au film results in the uncertainties of ~ 5 nm, $\sim 10^\circ$ and $\sim 40^\circ$ for λ_{TP} , ψ and Δ , respectively, as shown in Fig. 4, and the 2° uncertainty for $\theta_i = 65^\circ$ results in the uncertainties of ~ 6 nm, $\sim 1^\circ$ and 10° for λ_{TP} , ψ and Δ , respectively, as shown in Fig. 5. Therefore, the uniformity of Au thickness and the systematic error of θ_i may contribute to the different λ_{TP} , ψ and Δ between the experimental and simulation results shown in Fig. 3. The λ_{TP} also depends on metal's plasma frequency [19]. Therefore, other than the thickness and the measuring angle divergence, the dielectric constant of Au could also be a factor to cause the deviation from measurement to simulation results. However, the deposited gold film could be slightly different from the database.

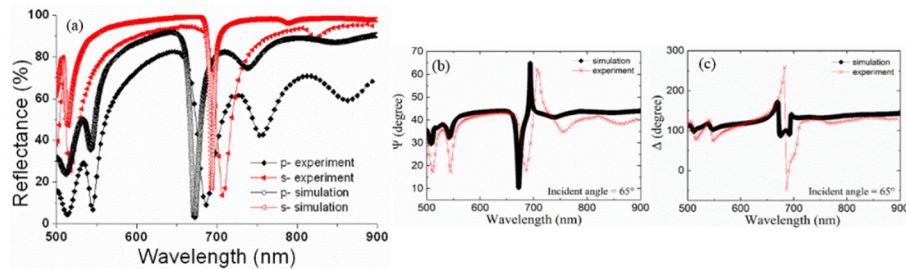


Fig. 3. Experimental and simulation results of (a) reflectance spectra (b) ψ and (c) Δ for the TP device in the air environment at $\theta_i = 65^\circ$.

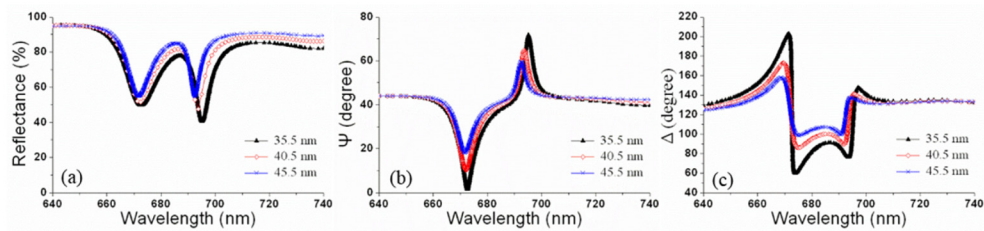


Fig. 4. The simulation results of (a) reflectance spectra (mean of p and s) (b) ψ and (c) Δ for the TP device in the air environment with different Au thicknesses at $\theta_i = 65^\circ$.

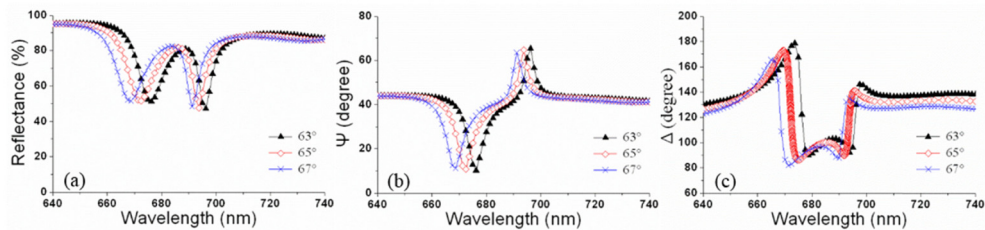


Fig. 5. The simulation results of (a) reflectance spectra (mean of p and s) (b) ψ and (c) Δ for the TP device in the air environment at different incident angles.

The changes of ψ and Δ , $\delta\psi$ and $\delta\Delta$, with the ambient environment changed from air to CO_2 at $\theta_i = 65^\circ$ are simulated as shown in Figs. 6(a) and 6(b), respectively. $\delta\Delta$ and $\delta\psi$ have the maximum absolute values $\sim 1.5^\circ$ and $\sim 0.25^\circ$, respectively. $\delta\Delta$ shows a better sensitivity for detecting the change of ambient index than $\delta\psi$. Therefore, we use the $\delta\Delta$ for further detection

application. The $\delta\Delta$ also depends on the wavelength, and the wavelength with the maximum value of $\delta\Delta$, λ_{max} , is chosen for studying the sensitivity. The maximum absolute value of $\delta\Delta$ is $\sim 1.5^\circ$ at $\lambda_{max} = 672$ nm as shown in Fig. 6(b).

Because the applied ellipsometer has the limited resolutions in wavelength and θ_i , we investigate the sensitivity of the proposed TP devices theoretically for the following discussion. The sensitivity $\delta\Delta$ can be improved by properly selecting several parameters, such as θ_i and PC structure. Simulation results of $\delta\Delta$ as a function of wavelength at different θ_i are shown in Fig. 7, where $\lambda_c = 730$ nm and $t_{TiO_2} = 239$ nm. It is seen that when the ambient environment is changed from air to CO_2 , the maximum $\delta\Delta$ depends on the θ_i . The $\delta\Delta$ and the corresponding λ_{max} as a function of wavelength at different θ_i are shown in Fig. 8. A maximum value $\delta\Delta \sim 2.0^\circ$ at $\lambda_{max} = 703$ nm is obtained when θ_i is near 50° . We also found that the structure of the PC, including t_{TiO_2} and λ_c , produces an influence on the sensitivity. Simulation results of $\delta\Delta$ and the corresponding λ_{max} as a function of t_{TiO_2} are shown in Fig. 9, where $\theta_i = 65^\circ$ and $\lambda_c = 730$ nm. The maximum value of $\delta\Delta$ is $\sim 12^\circ$ at $\lambda_{max} = 664$ nm when $t_{TiO_2} = 230$ nm.

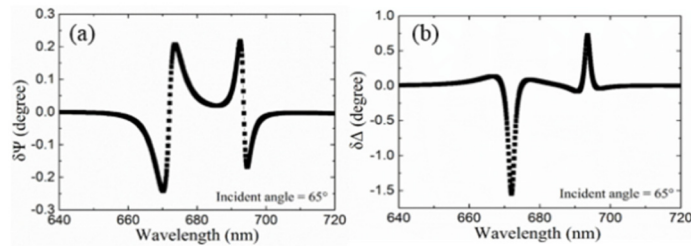


Fig. 6. Simulation results of SE parameters ψ and Δ for the TP device at $\theta_i = 65^\circ$ when the ambient environment is changed from air to CO_2 .

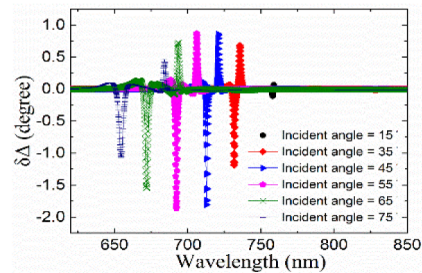


Fig. 7. $\delta\Delta$ as a function of the wavelength at different incident angles, where $\lambda_c = 730$ nm and $t_{TiO_2} = 239$ nm.

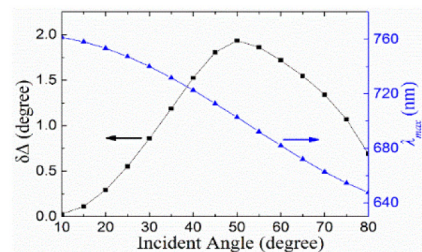


Fig. 8. $\delta\Delta$ and the corresponding λ_{max} as a function of the incident angle, where $\lambda_c = 730$ nm and $t_{TiO_2} = 239$ nm.

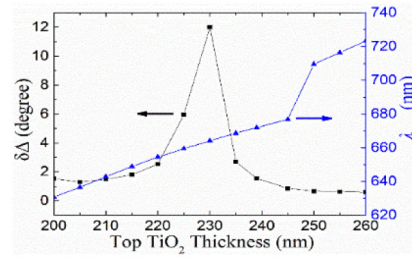


Fig. 9. $\delta\Delta$ and the corresponding λ_{max} as a function of t_{TiO_2} , where $\theta_i = 65^\circ$ and $\lambda_c = 730$ nm.

The λ_c can be adjusted by varying the thicknesses of the n_H and n_L films [19]. Simulation results of $\delta\Delta$ and the corresponding λ_{max} as a function of λ_c are shown in Fig. 10, where $t_{TiO_2} = 239$ nm and $\theta_i = 65^\circ$. The maximum value of $\delta\Delta$ is $\sim 34^\circ$ at $\lambda_{max} = 706$ nm as λ_c is 810 nm. The deposited thickness of each film in TP device may not be identical to the theoretical design due to the uncertainty of fabrication depending on the applied facility. If there is $\pm 1\%$ error in the final result of λ_c ($\lambda_c = 810$ nm), the $\delta\Delta$ falls in the range between $\sim 34^\circ$ and $\sim 20^\circ$ according to Fig. 10. Therefore, a sensitivity ($\delta\Delta/\delta n = 20^\circ - 34^\circ/0.00017$) in the range between 1.2×10^5 $^\circ/\text{RIU}$ and 2×10^5 $^\circ/\text{RIU}$ is obtained for the proposed TP device when the ambient environment is changed from air to CO₂. The resolutions of the commercial rotational stage and spectrometer are better than 0.1 $^\circ$ and 0.1 nm, respectively. Therefore the influences of the uncertainties from θ_i and wavelength on sensitivity is less than 10% according to the Figs. 8 and 10.

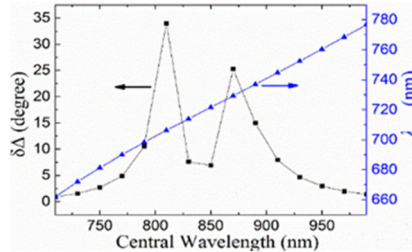


Fig. 10. $\delta\Delta$ and λ_{max} as a function of the central wavelength, where $t_{TiO_2} = 239$ nm and $\theta_i = 65^\circ$.

Phase-sensitive SPR and the detection limits are well described in the recently published articles [11,12]. The sensitivity of SPR depends on many factors, such as measurement geometry and instrumental and environmental noises [12]. Our applied commercial ellipsometer has noisy characteristics in terms of their stability, $\sim 0.2^\circ$. Based on this phase stability, the refractive index resolution of $\sim 10^{-6}$ RIU ($0.2^\circ/(\sim 2 \times 10^5$ $^\circ/\text{RIU})$) for the present design is obtained if only the instrumental noise is considered. The RI resolution can be further improved if the phase resolution of an instruments can be improved to $\sim 0.001^\circ$ by special designed low-noisy schemes [11,12,20].

4. Conclusions

In summary, a refractive index sensing concept of a TP device by using SE is proposed. The sensing performance can be designed and improved by adjusting the λ_c , the t_{TiO_2} and θ_i . A detection sensitivity of $\sim 2 \times 10^5$ $^\circ/\text{RIU}$ can be obtained for the proposed TP device when the ambient environment is changed from air to carbon dioxide, where $\lambda_c = 810$ nm, $t_{TiO_2} = 239$ nm, and $\theta_i = 65^\circ$. The main scientific contribution of this work is to provide the design rule for TP phase sensor. Comparing to Kretschmann–Raether prism geometry, TP sensor has the advantage in fabrication, low cost, and easy set-up.

Funding

Ministry of Science and Technology of Taiwan (MOST 103-2112-M-009-013-MY3 and MOST 105-2221-E-009-096-MY2).

Acknowledgments

We thank the anonymous reviewers for their constructive comments.